Landscape and Urban Planning 274 (2026) 105695

Contents lists available at ScienceDirect

Landscape and Urban Planning

journal homepage: www.elsevier.com/locate/landurbplan

Risk assessment in the Pyrocene – Rapid changes in models and predictions complicate US policies to prioritize forest and fuel management

Alan A. Ager [a,*], Michelle A. Day [a], Cody R. Evers [b], John B. Kim [c], Becky K. Kerns [d], Chris D. Ringo [e]

[a] USDA Forest Service, Rocky Mountain Research Station, Missoula Fire Sciences Lab, Missoula, MT USA
[b] Portland State University, Department of Environmental Science and Management, Portland, OR USA
[c] USDA Forest Service, Western Wildland Environmental Threat Assessment Center, Corvallis, OR USA
[d] USDA Forest Service, Pacific Northwest Research Station, Corvallis, OR USA
[e] Oregon State University, College of Agricultural Sciences, Corvallis, OR USA

HIGHLIGHTS

- Newer fire simulations for the US predict increased building exposure.
- Predicted exposure was substantially higher than observed.
- High exposure locations were consistent earlier simulations.
- Updates to ignition density, fuels, and buildings were contributing factors.
- Risk assessments need frequent updates to keep pace with changing fire regimes.

ARTICLE INFO

Keywords:
Wildfire
Wildfire simulation
Building exposure
FSim
Fire modelling
Wildland interface

ABSTRACT

Increased wildfire activity in the US motivated the USDA Forest Service to update national wildfire simulation data used for risk assessment and prioritizing wildland fuel reduction programs. The update (FSim-2020 to FSim-2023) included revised data on fuels, ignition frequency, fire weather, and recalibration of the FSim model. We overlayed the new simulated fire perimeters with the most recent building footprint data to examine the change in magnitude and spatial patterns of estimated building exposure. We found that the update to FSim-2023 resulted in a 61% increase in simulated building exposure in the East, and a decline of −9% in the West compared to FSim-2020. Overall, Forest Service priorities for management investments at the 100,000-ha scale were consistent between the two simulations in the West, but less so for the East, with newer simulations suggesting that a substantially greater area would require treatments to address the same level of exposure. Fire return level analysis indicated that differences between the prior and newer simulated building exposure varied across predicted recurrence intervals and fire size. Changes in building exposure were related to increases in ignition frequency, burn probability and building counts. A potentially important finding was the overestimation of simulated building exposure compared with observed (+112% West, +790% East) for the same approximate time period. One probable cause for the overestimation was the resampling of the LANDFIRE 30 m to the FSim 270 m, which resulted in a substantial reclassification of non-burnable to burnable pixels, particularly in and around the urban interface. The study underscores the importance of continued federal investment in risk assessment technology and data to keep pace with the rapid growth in wildfire extent and severity under evolving wildfire management policy.

* Corresponding author.
E-mail address: alan.ager@oregonstate.edu (A.A. Ager).

https://doi.org/10.1016/j.landurbplan.2026.105695
Received 1 May 2025; Received in revised form 27 April 2026; Accepted 15 May 2026
Available online 23 May 2026

1. Introduction

Land management agencies in the US and elsewhere are rapidly expanding their investments in wildland fire risk assessment technologies in response to the growing frequency of wildfire disasters. These assessments now underpin decisions by public and private entities to develop mitigation policy across a wide range of vegetation systems and governance contexts (e.g., BLM, 2024; Bunzel et al., 2023; Dillon et al., 2023; McEvoy et al., 2023; Scott et al., 2020; USGS, 2024; Zuzak et al., 2023). Rapid improvements in both data and models have helped mainstream the use of risk products with a particular attention to predicting human community disasters (First Street Technology, 2024; Oliveira et al., 2021; USDA Forest Service, 2024). At broader scales, risk assessments are also increasingly being used for prioritizing forest and fuel management investments across federal, state, local, and non-governmental lands for both ecological restoration and risk objectives (Ager et al., 2021c; Dye et al., 2021; McEvoy et al., 2021; Oliveira et al., 2021; USDA Forest Service, 2022). Many of the same risk assessment technologies used by public land management agencies are also widely used by the insurance and re-insurance industries to set premiums and work with homeowners to improve structure survival in the event of a wildfire (Auer, 2024; Hazra and Gallagher, 2022).

Wildfire risk assessment technologies incorporate a wide range of analytical methods (Oliveira et al., 2021), with Monte Carlo fire simulation models among the core tools for predicting future fire occurrence and the effects of wildland fuel modification treatments on fire behavior (Ager et al., 2011). Large numbers of simulated fires (e.g., millions) are used to map burn probability and flame length to estimate risk and exposure to a wide range of social and ecological values (Ager et al., 2019a; Alcasena et al., 2019; Braziunas et al., 2020; Evers et al., 2019; Parisien et al., 2020b). Despite many known issues with large fire simulation models (Adams and Neumann, 2024; Cruz and Alexander, 2013; Parisien et al., 2020a), their application to map risk and exposure and prioritize fuel management investments continues to expand in the US and other areas faced with growing wildfire-caused losses. Multiple countries have now employed wildfire simulation to generate large-scale maps of burn probability and intensity, and combined these outputs with building location and other values data to map exposure and wildfire risk (Ager et al., 2019b; Alcasena et al., 2021; Alcasena et al., 2018; Chen et al., 2024; McEvoy et al., 2023; Palaiologou et al., 2022; Price et al., 2015; Salis et al., 2021).

Despite the growing application, there are many challenges to the current risk calculus that were not envisioned in the quantitative wildfire risk framework first proposed by Finney (2005) and later operationalized for federal fuel reduction projects (Ager et al., 2007). Non-stationary fire regimes (Abatzoglou et al., 2021; Jones et al., 2022; NOAA, 2023), social and ecological diversity of fire-prone areas (Essen et al., 2023; Hamilton et al., 2024), and extreme events that account for the bulk of the loss (Abatzoglou et al., 2023; Ager et al., 2021a; Berchtold et al., 2025; Hulse et al., 2016; Naser and Kodur, 2025), all contribute to uncertainty in estimating and mapping wildfire risk at large scales. In particular, rapid changes in fire regimes in many regions of the globe are likely to outpace the frequency at which national-scale risk assessments are updated, creating a situation where priorities and decisions are being made on yesterday's risk. This includes updates to all risk subcomponents, including spatial data on human and ecological values, simulated wildfire likelihood and intensity, and wildfire vulnerability in developed areas. A further challenge to the risk science community concerns how complex risk products are communicated and interpreted by landowners and public land management planners (Santo et al., 2022).

A recent major update to the US national wildfire simulation (Dillon et al., 2023) and revised building location data (Microsoft, 2018, 2020) presented the opportunity to examine how simulated wildfire exposure to buildings (where fires start and spread to expose buildings) changed over the past 5–10 years, and the resulting effect on USDA Forest Service (USFS) priorities for forest and fuel management. The updated fire simulations included changes to key parameters that control simulated fire distributions, such as more recent fire weather, fire history, and ignition location data, as well as updates to vegetation and fuels (Dillon et al., 2023; LANDFIRE, 2017, 2020; Short et al., 2020a). Given that the update was part of a larger US government effort to continuously improve wildfire risk technology, and the importance of risk products for prioritizing US federal fuel management, we asked: 1) How did simulated building exposure change between the two datasets, and are those changes comparable to actual observed exposure as determined from recorded wildfire perimeters? 2) How have these changes altered locations identified by the USFS as the highest priority for reducing wildfire exposure as identified in prior work (Ager et al., 2021b) based on the earlier simulations? and 3) What factors in terms of data updates and modeling methods explain these differences? We discuss implications of the findings for risk-based policy and planning and the need to continually refine risk modeling to reflect changing fuels, weather, and fire regimes to improve model performance.

2. Methods

2.1. Study area

The study was conducted at three spatial extents including the conterminous USA (CONUS), Western US, and Eastern US. The Western US extent included 11 western US states: Arizona (AZ), California (CA), Colorado (CO), Idaho (ID), Montana (MT), Nevada (NV), New Mexico (NM), Oregon (OR), Utah (UT), Washington (WA), and Wyoming (WY). The Eastern US was defined as the remaining 37 states in CONUS. To assess landscape-scale changes, the study used the fireshed framework (Ager et al. 2021), a nested spatial framework that organizes landscape variation in wildfire risk to developed areas into containers across CONUS. Firesheds are the broad 100,000-ha scale unit for USFS prioritization (Evers et al., 2024)(Supplementary Material Fig. S1).

2.2. Wildfire simulation

We used burn probability grids and wildfire perimeters from two versions of FSim national wildfire simulations (Dillon et al., 2023; Short et al., 2020a). FSim consists of modules for weather generation and large-fire ignition, growth and suppression (Finney et al., 2011; Finney et al., 2025). The model is described in detail in Finney et al. (2011) and is widely used in the US for wildfire risk assessments at local, regional, and national scales for present day conditions (Dillon, 2024; Scott et al., 2024) and the future (Dye et al., 2023; Dye et al., 2024; Riley et al., 2025).

Tens of thousands of contemporary wildfire seasons are generated by FSim based on relationships between recent historical Energy Release Component (ERC; Bradshaw et al., 1983) and recent historical fire occurrence. ERC measures the potential heat (BTU/ft) in the flaming front of a fire and is used in the US National Fire Danger Rating System (Bradshaw et al., 1983). Time series analysis is used to estimate trends and variability in daily ERC, including temporal autocorrelation, to simulate synthetic fire seasons with the same statistical properties of historical weather, while incorporating variability in the daily average and trend. Ignition probability is based on historical occurrence and sampled by FSim in a grid format. Weather conditions derived from the synthetic fire seasons are used to simulate fire growth with the minimum travel time (Finney, 2002) algorithm. Fire growth occurs on days that meet a threshold ERC based on empirically derived wind and fuel moisture. Fire containment is controlled by a statistical model that estimates the probability of containment and a "perimeter" trimming function that simulates the effects of suppression actions on fire growth and shape (Dillon et al., 2023; Finney et al., 2009; Finney et al., 2025).

We compared two successive versions of simulation outputs covering CONUS published on the Forest Service Research Data Archive in 2020

(Short et al., 2020a) and 2023 (Dillon et al., 2023). Input data for both 2020 and 2023 simulations were obtained from multiple sources with different vintages (Fig. 1, Table 1). Documented changes in the modeling methodology between 2020 and 2023 are outlined in the Supplementary Material. Hereafter, the simulation versions, their outputs, and associated analyses will be referenced as FSim-2020 and FSim-2023. Outputs from both versions were stratified by 128 geographic units called "pyromes", areas of relatively homogeneous seasonal patterns of fire weather and fuel moisture (Short et al., 2020b)(Supplementary Material Fig. S1). Ignition probability grids were generated from a national fire occurrence database (Short, 2017, 2022). Note that pyromes have no relationship to fireshed boundaries since the latter are determined by the source of wildfire exposure to buildings (Supplementary Material Fig. S1). For each pyrome, between 10,000 and 100,000 fire seasons were simulated using stochastically generated weather (Finney et al., 2011). The FSim-2020 and FSim-2023 simulations contained 79 million and 183 million fire events (hereafter fires), respectively. This increase reflects both changes in observed ignition frequency and an increased number of simulated fire seasons to improve accuracy. Outputs included annualized burn probability and conditional flame length probability grids (270-m resolution; published in Short et al. 2020; Dillon et al. 2023), and ignition points and fire perimeters (unpublished). The FSim-2020 simulations were evaluated in Ager et al. (2021c) and both datasets in Carlson et al. (2025).

2.3. Simulated and observed annual area burned

Simulated average annual area burned was calculated by multiplying the mean fireshed burn probability (BP) by the area in each fireshed and summing the totals across all firesheds at the CONUS and Western versus Eastern spatial extents. Observed area burned was derived from the Fire Occurrence Database (Short 2022) by summing fire size by year and averaging across years (AK, HI, and PR were excluded) for the same spatial extents.

Table 1
Input data sources assembled to produce the FSim simulations in 2020 and 2023 and map wildfire transmission to buildings using the Microsoft building footprints published in 2018 and 2020.

Data	Version FSim-2020	FSim-2023
FSim fire event simulations	2020 (Short et al., 2020a)	2023 (Dillon et al., 2023)
FSim Energy release component, wind speed, direction and fuel moisture	1972–2012 (see Dillon et al., 2023)	2004–2018 (see Dillon et al., 2023)
LANDFIRE Surface and canopy fuels[a]	2014 (LANDFIRE, 2017)	2020 (LANDFIRE, 2020)
FSim ignition frequency and fire size thresholds	1992–2015 (Short, 2017)	1992–2020 (Short, 2022)
Historical area burned	1992–2015 (Short, 2017)	2006–2020 (Short, 2022)
Building locations[b]	2018 (Microsoft, 2018)	2020 (Microsoft, 2020)
Historical building exposure	1992–2015 MTBS intersected with buildings (MTBS, 2020)[c]	2006–2020 MTBS intersected with buildings (MTBS, 2024)
Historical building loss	NA	1999–2020 ICS-209 (St Denis et al., 2020)

[a] Details on changes in the LANDFIRE data vintages are documented in the Supplementary Material.
[b] The matching of the simulations with building footprint data was approximate due to the variable data vintages in the respective data sets. Note that most building footprints (56%) date from 2019 to 2020, the remainder date from imagery from a range of dates, averaging 2012.
[c] Note that the comparison between the FSim-2020 simulated data and MTBS observed data for the 2000–2018 is presented in Ager et al. (2021a).

2.4. Simulated building exposure

Wildfire transmission to buildings (hereafter building exposure) was calculated by first intersecting vector building datasets created by the

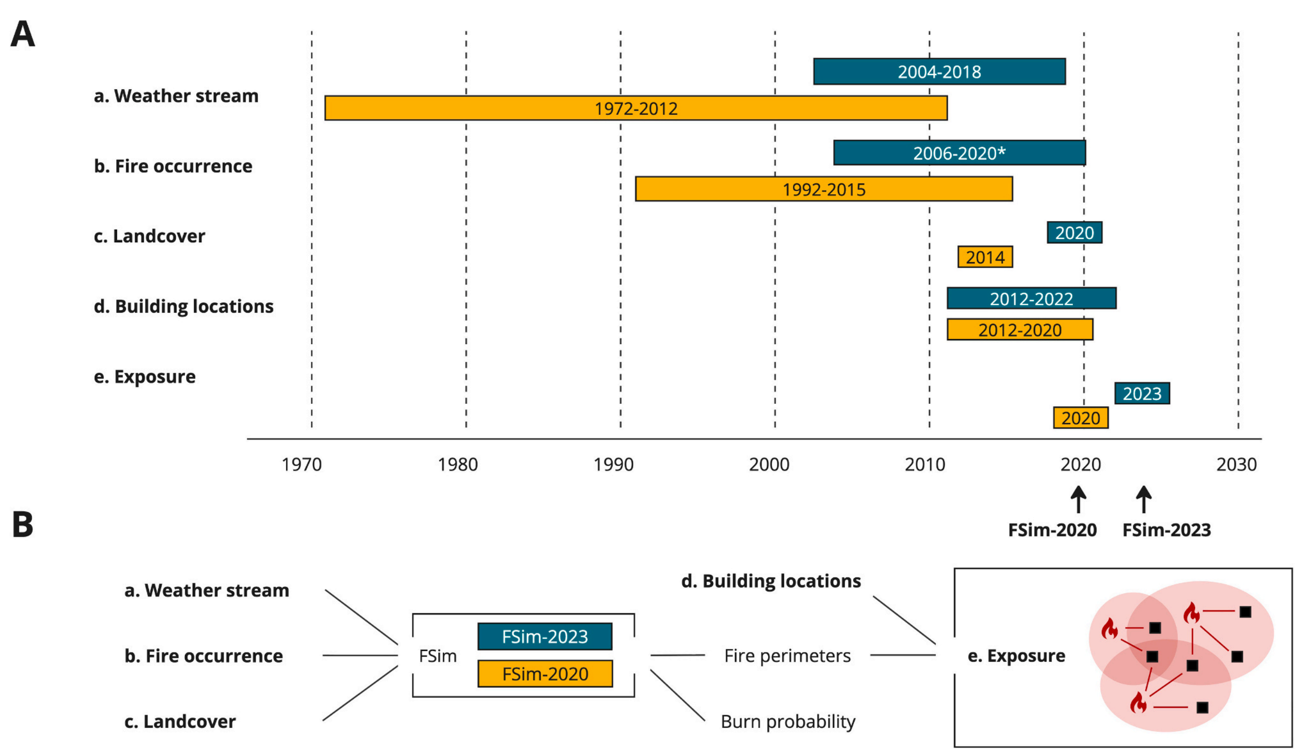

Fig. 1. Time periods for the respective input data assembled to simulate wildfires and building exposure from the FSim-2020 and FSim-2023 data sets (A) and overview of process used to estimate wildfire transmission to buildings (building exposure) (B). For the latter, FSim fire event perimeters (pink ovals in inset) were intersected with the Microsoft building location data (black squares) and building counts attributed to ignitions (flame symbol) and smoothed across all ignitions to estimate simulated building exposure. Data sources are enumerated in Table 1. *1992–2020 time period was used for ignition density and large fire size thresholds.

Bing Maps team at Microsoft (Microsoft, 2018, 2020) with simulated fire perimeters (Fig. 1 inset). This process assigned a count of buildings exposed within each simulated fire perimeter. We then attributed the ignition point associated with the fire perimeter with the building count to create a point map of the source of building exposure events. This attributed ignition dataset was used to create a 90 m smoothed building exposure raster using inverse distance weighting with a search radius of 2500 m and a power of 0.5 (Ager et al., 2021c; Bunzel et al., 2023). The resulting raster represented the total building exposure from all simulated fires that burned in that location. To convert to an expected annual value (i.e., account for the probability of a fire at that location) we created a simulated ignition probability raster (ignitions ha^{-1} yr^{-1}) using the ArcGIS point density tool, with a 2500 m circular search radius and the population field set to ignitions per year (Ager et al., 2021b; Ager et al., 2021c). The exposure raster and ignition probability raster were then multiplied to create a final smoothed building exposure raster, in which each cell represents the expected annual number of buildings exposed by wildfire igniting in the pixel (Bunzel et al., 2023, 2026). Note that the resulting grid describes the potential transmission of fire from the pixels to buildings (as opposed to quantifying exposure within the pixel, or *in situ* exposure).

The above process was repeated for the 2018 building data (n = 123,970,269) paired with the 2020 FSim outputs, and the 2020 building data (n = 128,842,736) paired to the 2023 FSim data to create the FSim-2020 and FSim-2023 building exposure datasets, respectively.

2.5. Observed building exposure

Observed building exposure for time periods that matched the two simulation data sets (Fig. 1) was determined by intersecting the Monitoring Trends in Burn Severity wildfire perimeters (MTBS, 2024) with the Microsoft building footprints. The number of buildings exposed to fire was then summed for each year from 1992 to 2020 and averaged across all years for two time periods depending on the simulation data set (Table 1). Since MTBS does not record fires < 404 ha in the West and < 202 ha in the East, simulation datasets were filtered for fires greater than the respective fire size threshold based on western or eastern states to match historical data from MTBS. We used this size threshold to define large versus small fires when exploring patterns of exposure with fire size. We also used data compiled in St Denis et al. (2020) from the ICS-209 reports to analyze the relationship between fire size and historical building damage and loss in the Western US.

2.6. Analysis

2.6.1. Simulated building exposure

To assess the impact of the updated simulations we performed multiple analyses of simulated building exposure and area burned in the FSim-2020 and FSim-2023 data over a range of scales including firesheds, Western US, Eastern US, and CONUS. We first compared the average simulated FSim-2020 and FSim-2023 annual building exposure and area burned with observed (historical) values over an approximately similar time span (Table 1). These summary data provided a two-way comparison of simulated versus observed data sets for both FSim-2020 and FSim-2023 area burned and building exposure. We also compared simulated with observed building exposure data for large fires, and between simulation versions for small fires (see above). These comparisons used boxplots to understand the magnitude of the annual variability (among fire seasons) relative to the difference in the mean values. Note that changes reported could be the result of conditions changing on the ground (e.g., impact of disturbance events) or improvements to remote sensing, or model parameters that result in different estimates of fuel conditions or burn probability.

We then examined whether the differences in area burned and building exposure between FSim-2020 and FSim-2023 were evenly distributed among specific event levels and statistically significant using return-level graphs. Return-level graphs are a standardized risk assessment tool for quantifying the frequency and magnitude of natural disasters including floods, earthquakes, and hurricanes (Ager et al., 2021a; Coles et al., 2001; Lambert et al., 1994; Mills et al., 2018; Sajjad et al., 2020). Return level plots describe expected time between events exceeding a given threshold, in this case a fire season with a specific level of annual burned area or building exposure. Note that return level plots are not the ecological fire return interval commonly used to characterize different fire ecology systems. For this purpose we used the first 10,000 fire seasons within each pyrome from the two versions and fit a generalized pareto distribution (Schoenberg et al., 2003) to the tail-end distribution of each using the *extRemes* package in R (Gilleland and Katz, 2016) to estimate six fire return levels (every 5, 10, 25, 50, 100 and 200 years) for annual area burned and building exposure for the Eastern and Western US and CONUS. The statistical significance was assessed by the lack of overlap between 95% confidence intervals for estimated area burned and building exposure levels for FSim-2020 and FSim-2023.

To contrast fine scale spatial patterns of building exposure for the FSim-2020 and updated FSim-2023 wildfire simulations (Short et al. 2020; Dillon et al. 2023, respectively), we created CONUS scale maps rendered based on average annual building exposure using the smoothed 90-m resolution maps described above. Class breaks were based on average annual building exposure at 200, 6.25, 1.25, 0.5 and 0.1 buildings exposed based on ignitions per 10,000 ha of area for high, moderate, moderately low, low, and very low respectively based on the FSim-2020 data. The FSim-2023 map used the same class breaks and map symbology.

2.6.2. Prioritization

To understand how the updated simulations might affect USFS priorities established at the larger fireshed scale in prior work (Ager et al., 2021b) we summed the 90 m building exposure data to firesheds (ca. 100,000 ha) and mapped the average change in simulated building exposure between the two simulation data sets. We then ranked the firesheds based on total simulated building exposure (highest to lowest) and compared these rankings to the prior ones based on the FSim-2020 version of the data (Bunzel et al., 2023). We used the sorted fireshed list to calculate the cumulative area responsible for increasing amounts of building exposure (i.e., the land base where the exposure originated, see (Ager et al., 2021c)) and then identified the land base required to treat specific levels of exposure.

2.6.3. Contributing factors

Finally, we explored how key inputs (fuels, building counts, ignition frequency) changed between FSim-2020 and FSim-2023 using fireshed mean values. Ignition frequency was obtained from the FSim input files (data not publicly available; Dillon et al., 2023; Short et al., 2020a). We also examined changes in burn probability, an intermediate output that is influenced by multiple other factors related to fire ignition and spread. Changes in mapped fuels were assessed by calculating the percentage of fuels within each fireshed in coarse fuel groupings (grass, shrub, timber, and non-burnable) for the vintage of the fuel data used in each simulation version (LANDFIRE, 2017, 2020) (Supplementary Material). To quantify the relative influence of the above explanatory variables on changes in simulated building exposure, we fit log–log regression models using the errorsarlm function in the R package *spatialreg* (Bivand and Piras, 2015). These models use differences in the log values of both the dependent variable (building exposure) and independent variables (burn probability, ignition density, building counts, and grass, shrub, timber, and non-burnable fuel classes) to estimate the percent change in the dependent variable for a one percent change in the independent variable while accounting for spatial autocorrelation among firesheds. To control differences in magnitude of exposure among firesheds, we also included the log transformed FSim-2020 exposure. All values were standardized as z-scores to allow comparison among potential drivers. Separate models were fit for the entire CONUS, Western US, and Eastern

US. Spatial neighbors were defined among firesheds using queen contiguity of fireshed polygons, with a snap tolerance of 100 map units to account for minor boundary mismatches. For any firesheds with no contiguous neighbors, we assigned neighbors using the 8 nearest fireshed centroids. Spatial weights were then row-standardized before model fitting. We examined pairwise correlations and variance inflation factors and found no evidence of multicollinearity. We also evaluated spatial autocorrelation using Moran's I tests on residuals from the corresponding non-spatial linear models and found substantial residual spatial autocorrelation, which supported the use of spatial error regression. Finally, we retested Moran's I on residuals from the spatial error models and found no evidence of remaining spatial autocorrelation.

3. Results

3.1. Effect of updates on simulated area burned and building exposure and comparison with observed

Annual area burned estimated from wildfire simulations increased from 1.94 to 2.72 million ha per year from FSim-2020 to FSim-2023, or a 40% increase for CONUS (Table 2). The observed area burned tabulated from historical data increased 38% during the same approximate time periods (1992–2015 and 2006–2020, Tables 1-2). Building exposure estimated from wildfire simulations also increased across CONUS from the FSim-2020 to FSim-2023 simulations from 43,559 to 52,751 buildings per year, or +21% (Table 3). The increase in simulated building exposure was entirely in the Eastern US (61%) with a decline of 9% in the Western US. Observed exposure for CONUS tabulated from historical fire perimeters also increased (32%), with the bulk of the increase in the West (43% in the West vs. 7% in the East, Table 3). In sum, at the CONUS scale the changes in the observed and simulated building exposure across data vintages/time periods showed a reasonably similar increase, but not when examined at the sub-CONUS scale where changes in building exposure data were not consistent with observed. More detailed examination of the change in building exposure between the FSim-2020 and FSim-2023 simulation data showed a consistent increase in exposure only for small fires (<405 ha in the West and < 202 ha in the East (MTBS, 2024)) mostly in the Eastern US (Fig. 2). This finding is consistent with observed building damage tabulated from ICS-209 reports (St Denis et al., 2020) showing a higher proportion of loss per ha burned for small fires (Supplementary Material Fig. S2).

Estimates of annual area burned from simulations compared with historical data showed close correspondence for both simulation datasets and across geographies (ranging between +2% and +10%) except for the Eastern US FSim-2023 comparison (+18% overestimation, Table 2). Despite a similar overall increase in both simulated and observed building exposure for CONUS between time periods, estimates of mean building exposure from simulation were higher than that calculated from observed fire perimeters for all three geographic scales (Table 3, Fig. 2), and more outlier fire seasons were evident in the simulation data. In the Western US, simulated exposure exceeded observed amounts for both FSim-2020 (+235%) and FSim-2023 (+112%). Overestimation was even more extreme in the Eastern US with simulated building exposure exceeding observed by 493% and 790% for the FSim-2020 and FSim-2023, respectively. Again, as noted above, the time stamps of the wildfire simulations and building footprints do not match exactly due to the multiple data sources and their respective collection dates used in the calculations (Fig. 1), but the magnitude of the overestimation suggests other factors are involved. Note also that the comparison of simulated to observed building exposure was limited to fires > 405 ha in the Western US and > 202 ha in the Eastern US to match historical data collection thresholds (see Methods) although Fig. 2 suggests that inclusion of the smaller fires would increase overestimation further.

Table 2
Statistics on annual area burned for the FSim-2020 and FSim-2023 simulations. See Table 1 and Fig. 1 for explanation of data sources.

Scale of comparison	Data vintage[a]	Annual area burned (millions ha) Observed	Simulated	Difference (Simulated-observed)
CONUS	FSim-2020	1.83	1.94	+6%
	FSim-2023	2.54	2.72	+7%
	Difference (FSim-2023-FSim-2020)	+38%	+40%	
Western US	FSim-2020	1.27	1.39	+10%
	FSim-2023	1.81	1.85	+2%
	Difference (FSim-2023-FSim-2020)	+43%	+34%	
Eastern US	FSim-2020	0.55	0.56	+2%
	FSim-2023	0.73	0.86	+18%
	Difference (FSim-2023-FSim-2020)	+33%	+55%	

[a] Data vintage indicates FSim simulation version and associated historical data calibration date ranges. FSim-2020 simulations used observed data from 1992 to 2015; FSim-2023 simulations used observed data from 2006 to 2020.

Table 3
Statistics on simulated and observed building exposure for the FSim-2020 and FSim-2023 simulations and Monitoring Trends in Burn Severity (MTBS, 2024) fire perimeters intersected with Microsoft building footprint (Microsoft, 2020) data. See Table 1 and Fig. 1 for explanation of the data sources.

Scale of comparison	Data vintage[a]	Annual building exposure (buildings per year) Observed	Simulated	Difference (Simulated-observed)
CONUS	FSim-2020	10,527	43,559	+314%
	FSim-2023	13,881	52,751	+280%
	Difference (FSim-2023-FSim-2020)	+32%	+21%	
Western US	FSim-2020	7,322	24,558	+235%
	FSim-2023	10,438	22,114	+112%
	Difference (FSim-2023-FSim-2020)	+43%	−9%	
Eastern US	FSim-2020	3,205	19,001	+493%
	FSim-2023	3,442	30,637	+790%
	Difference (FSim-2023-FSim-2020)	+7%	+61%	

[a] Data vintage indicates FSim simulation version and associated historical data calibration date ranges. FSim-2020 simulations used observed data from 1992 to 2015; FSim-2023 simulations used observed data from 2006 to 2020.

3.2. Effect of updates on simulated extreme events

Return-level plots for the two simulations described expected time between fire seasons exceeding a specific threshold, in this case levels of area burned or building exposure. The analysis of return level plots for the FSim-2020 and FSim-2023 simulations revealed significant differences in the distribution of fire seasons with specific levels of impacts. Annual area burned (Fig. 3A-C) was higher with FSim-2023 among all fire return levels and a slight tendency for higher magnitude at the longer return levels. For instance, Fig. 3A illustrates a fire season with at least 6.5 million ha burned per year once every 200 years for the FSim-2023 data, and about 5 million ha burned for the same time interval for FSim-2020. For the Eastern US (Fig. 3C), this trend was noticeably amplified for the longer (>100 yrs) simulated time to occur. These results are consistent with the observed increase in annual area burned since 2006 reported in Table 2 for all three spatial domains (Fig. 3A-C). Statistical significance between FSim-2020 and FSim-2023 simulations is inferred when the 95% CI around the interannual variation in burned area did not overlap for a given fire return level (Fig. 3).

Return-level graphs for building exposure showed the opposite

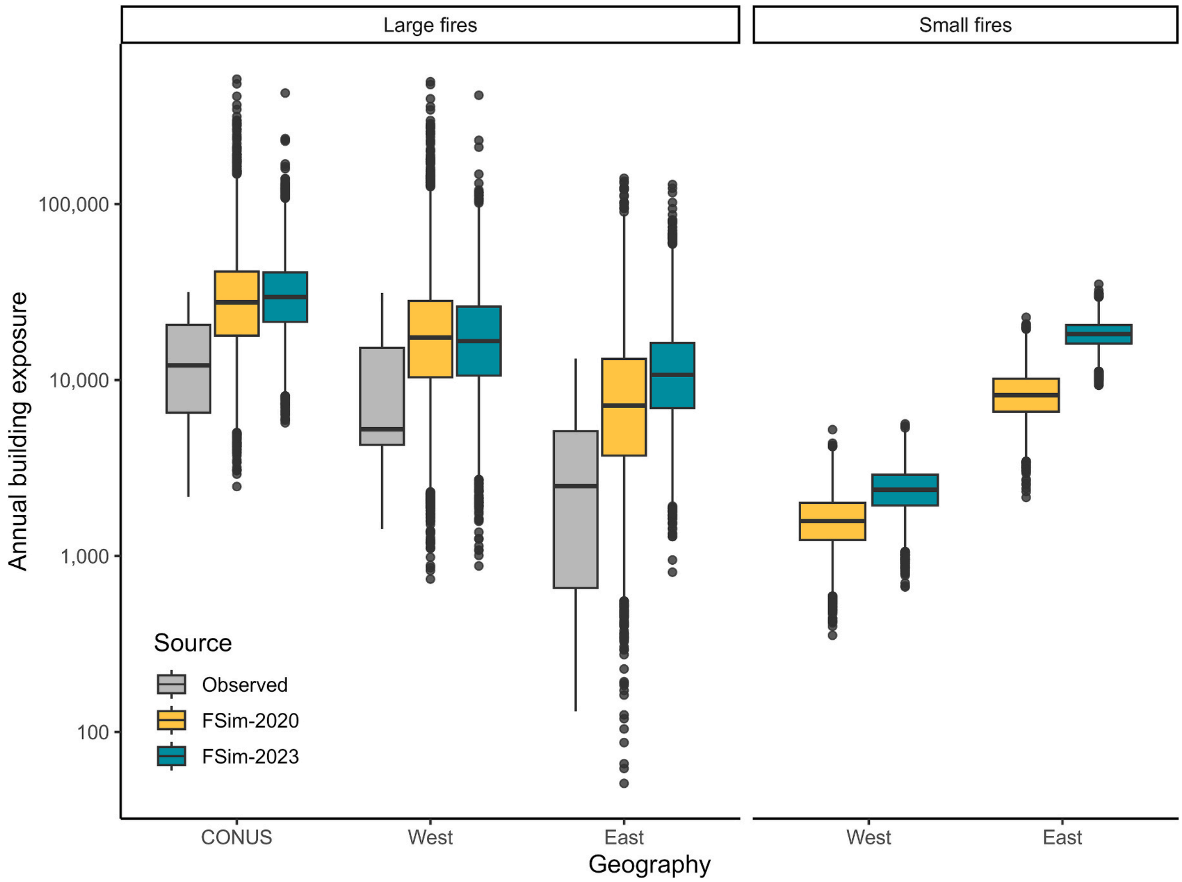

Fig. 2. Effect of fire size on the magnitude of change in estimated building exposure and comparison of estimated with observed. Observed annual building exposure was calculated from Monitoring Trends in Burn Severity (MTBS 2024) historical perimeters with simulated annual building exposure from FSim-2020 and FSim-2023 calculated for A) large and B) small fires in the conterminous US (CONUS) and Western and Eastern US. Large fires are defined as > 405 ha in the Western US and > 202 ha in the Eastern US based on MTBS definitions. Note that the definition of large fire used for calibration in FSim varies by pyrome based on historical fire size distributions but fires of all sizes are output by the model. Years for historical comparison are 2006–2020.

results as area burned with lower exposure in the FSim-2023 simulations for CONUS and the Western US (Fig. 3D-E), yet higher in the East (Fig. 3F, Table 3) for shorter return levels. However, the analysis showed that the difference in building exposure between the FSim-2020 and FSim-2023 simulations was significantly dependent on the magnitude of the simulated building exposure for a given fire season, especially for CONUS and the Western US where the magnitude of low occurrence (>50 yr return level), high building exposure years was substantially reduced in the FSim-2023 data (Fig. 3D-E). Overall, for CONUS and the Western US the most infrequent fire return levels have lower building exposure with FSim-2023. However, in the Eastern US this overall trend was reversed (Table 3), with higher building exposure observed with FSim-2023 for lower fire return levels (Fig. 3F).

3.3. *Effect of updates on the spatial distribution of simulated building exposure*

Spatial patterns of simulated building exposure for the FSim-2020 versus FSim-2023 data (Fig. 4) and the change in exposure (Fig. 5) revealed hotspots of both increased and decreased building exposure. Fig. 4 was created by smoothing ignition points that were attributed with building counts within the resulting fire perimeters at 90 m resolution (see Methods). Fig. 5 was created by aggregating the data in Fig. 4 to the fireshed scale (100,000 ha, (Evers et al., 2024)) to compare with prior reports (Ager et al., 2021b). In the Western US, the location of hotspots identified with FSim-2020 data were consistent with FSim-2023 data, and observed around the east Cascade, Siskiyou, and southern-central Sierra Mountain ranges, and in the wildlands surrounding the Los Angeles area. Smaller concentrated high exposure was also simulated for portions of the Sawtooth Mountains, Mogollon Rim, and Rocky Mountains east of Denver. Note that the building exposure results from ignitions located in the hotspots. Note also substantial increases in simulated exposure over large areas in the Central and Eastern US, including east Texas, Oklahoma Ozark Mountains, and especially the southern Appalachian States (Fig. 4A versus 4B).

Fireshed scale changes in the simulated exposure showed that although hotspots are apparent in the 90 m data for both FSim-2020 and FSim-2023, the updated simulations showed a decrease in exposure in many firesheds in coastal and southern California, central and south Arizona, Florida and elsewhere (Fig. 5). One third (2,560) of all firesheds were estimated to have a modest increase in exposure of at least 1 building per year. Approximately 5.9% of firesheds (452) exhibited an increase in exposure that exceeded 11 buildings per year (dark red, Fig. 5).

3.4. *Effect of the update on priority firesheds*

At the fireshed scale, we found that high priority firesheds (top 5%, Fig. 6, Table 4) remain largely stable, but potential efficiency of treatments declined from that previously reported. Specifically, when the updated simulated exposure data were used to prioritize firesheds as reported for the FSim-2020 simulations (Ager et al., 2021b), in general, the locations of the highest ranking firesheds (those with the most simulated building exposure) did not change between simulation versions (Fig. 6A versus 6B), particularly for the top 25% of firesheds across the Western US. For instance, 54% of firesheds that were ranked in the

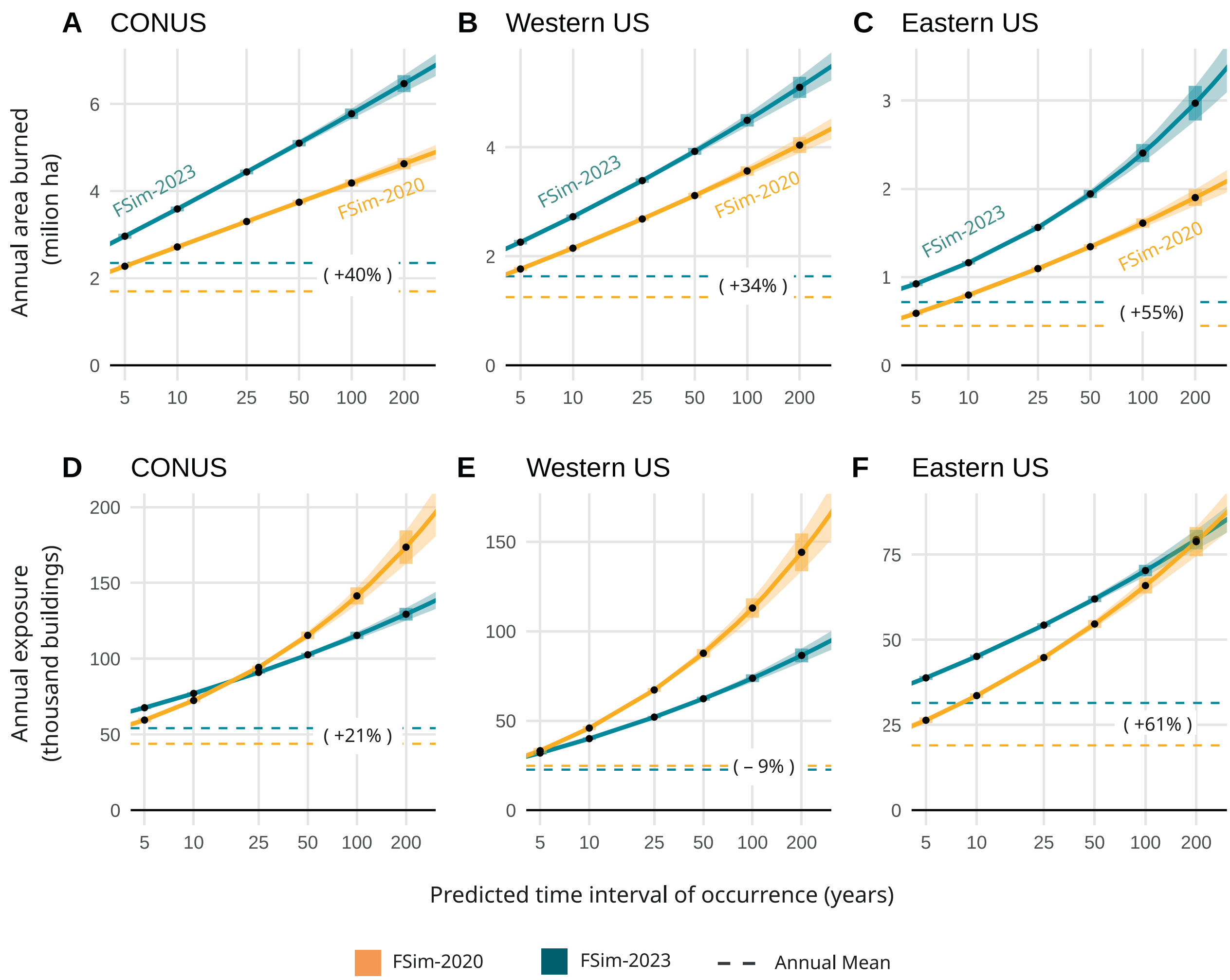

Fig. 3. Return-level plots showing the relationship between event magnitude and recurrence interval for simulated annual burn area (top row) and building exposure (bottom row) in the FSim-2020 and FSim-2023 datasets. Columns show results for the CONUS (left), Western US (middle), and Eastern US (right). Upward-sloping curves reflect the rarity of extreme fire seasons; parallel curves indicate consistent tail shape, while changes in slope or intercept reveal differences in how extreme events contribute to long-term averages. Seasonal averages reported in Tables 2 and 3 are shown as dashed horizontal lines. 95% confidence intervals (CI) are shown as ribbons. Vertical colored bars indicate the 95% CI for a given return period.

top 1% with FSim-2020 stayed in the top 1% with FSim-2023. Of the firesheds ranked in the top 25% with FSim-2020 (firesheds in the top four percentile bins in Fig. 6), 51% did not change ranks while 13% of firesheds increased rank, and 36% decreased in rank with FSim-2023 building exposure estimates. A more significant result was a substantial increase in the area that accounted for 80% of the total exposure, a benchmark reported in prior work (Ager et al., 2021b), that amounted to a 52 million ha increase from FSim-2020 to FSim-2023. The total building exposure associated with the top 10% of the area (77.8 million ha) decreased 12% for FSim-2023 versus FSim-2020 (Table 4). This means that the potential treatment leverage, i.e., the building exposure per area treated, declined in the newer data (Table 4) suggesting that significantly more area would need treatment (e.g., thinning, prescribed fire) within each fireshed to achieve the same level of potential exposure reduction based on the FSim-2020 data.

3.5. Factors associated with building exposure change

Regression analyses using fireshed mean data suggested that ignition frequency and burn probability were the main drivers for changes in annual building exposure across CONUS (Table 5) after accounting for baseline exposure, followed by changes in building counts. More specifically, the standardized coefficient for change in ignition frequency was roughly twice that for change in burn probability and about three times that for change in building count. Regionally, exposure change in the Western US was more strongly associated with changes in burn probability, with the burn probability coefficient roughly three times larger than both ignition frequency and building count. In the Eastern US, changes in exposure were most strongly tied to changes in ignition frequency, having 3.5 times the influence of burn probability and 1.7 times the influence of building count. In general, associations between increased exposure and changes in fuel types were weak and not statistically supported in the spatial error models, although there was marginal evidence in the Western US for an association with decreased shrub fuels. Scatterplots at the fireshed scale comparing key FSim-2020 versus FSim-2023 data showed in general increases in the modeled ignition frequency from FSim-2020 to FSim-2023 especially in the Eastern US (Fig. 7A) (see also Supplementary Material Figs. S3-S6). This likely contributed to the overall increase in burn probability (Fig. 7B) although many other parameters, especially modifications to fuels, could explain the increase (see below). Interestingly, building count showed little change from the update to the Microsoft building footprint data (Fig. 7C). Although the overall number of buildings increased from 125 million to 130 million (4%), building counts decreased for 29% of the firesheds, with the obvious outliers in the Western US (Fig. 7C). The scatterplot of simulated building exposure for firesheds in the Eastern US

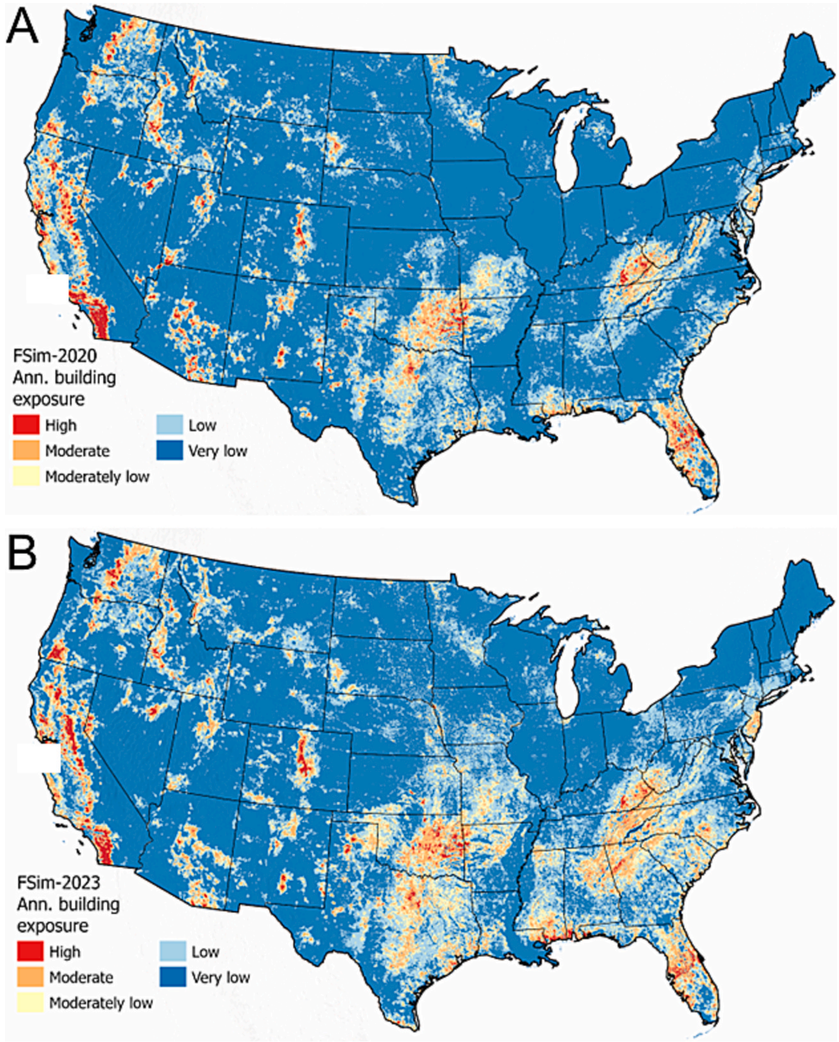

Fig. 4. Spatial patterns of estimated annual building exposure for the FSim-2020 (A) and updated FSim-2023 (B) raster (90-m pixel) datasets (Short et al. 2020; Dillon et al. 2023, respectively). Class breaks were based on average annual building exposure based on the FSim-2020 data. The FSim-2023 map used the same class breaks and map symbology. See Methods for additional details.

(Fig. 7D) shows a similar pattern of change for ignition frequency and burn probability, with the values more or less evenly dispersed above the line of no change. However, an entirely different pattern was observed for the Western US with a large number of firesheds having both increased and decreased average building exposure, suggesting other factors are driving the observed change. Further examination of the change in burn probability and ignition frequency for only firesheds with a decrease in exposure did not suggest a cause-and-effect relationship.

Analysis of the change in fuel type between the FSim-2020 and FSim-2023 simulations revealed large changes in classification and wide variation among firesheds (Supplementary Material, Fig. S7) and USFS regions (Table S1). These changes could be partly responsible for the increased burn probability and resulting building exposure, although the regression analysis described above showed little association with changes in fuels. Overall, the fuel type changes varied significantly among firesheds and thus generalizing the updated fuels in terms of spread rate and resulting burn probability was not possible.

4. Discussion

This work assessed the change in predicted building exposure from simulated wildfires in the US after recent updates to fuels, weather, and the re-calibration of the FSim large fire simulation model. The primary objectives of the work were to determine whether updates significantly changed previously reported spatial patterns and magnitude of simulated building exposure, and secondarily, USFS priorities for managing hazardous fuels to mitigate building loss in the wildland urban interface (WUI). A tertiary objective was to understand the major drivers in terms of input variables to the building exposure calculations. The result of the update was an increase in simulated annual area burned that closely mirrored the trend in observed wildfire over the same approximate time period. Simulated building exposure for the conterminous US was also coarsely consistent with trends in observed building exposure. However, there was a decrease in simulated building exposure for the West (−9%) and an increase for the East (+61%). Overall priorities for management investments at the fireshed scale remain largely consistent between the FSim-2020 and FSim-2023 simulations, although the latter outputs suggest that substantially greater area would require investments than previously estimated to treat the same level of exposure particularly in the Eastern US (Table 4). Changes in simulated building exposure were likely related to updates to multiple input variables (fuels, ignition frequency, and weather), with strong interactive effects at the fireshed scale.

Beyond these findings, a potentially important result was that the newer FSim-2023 simulated building exposure substantially

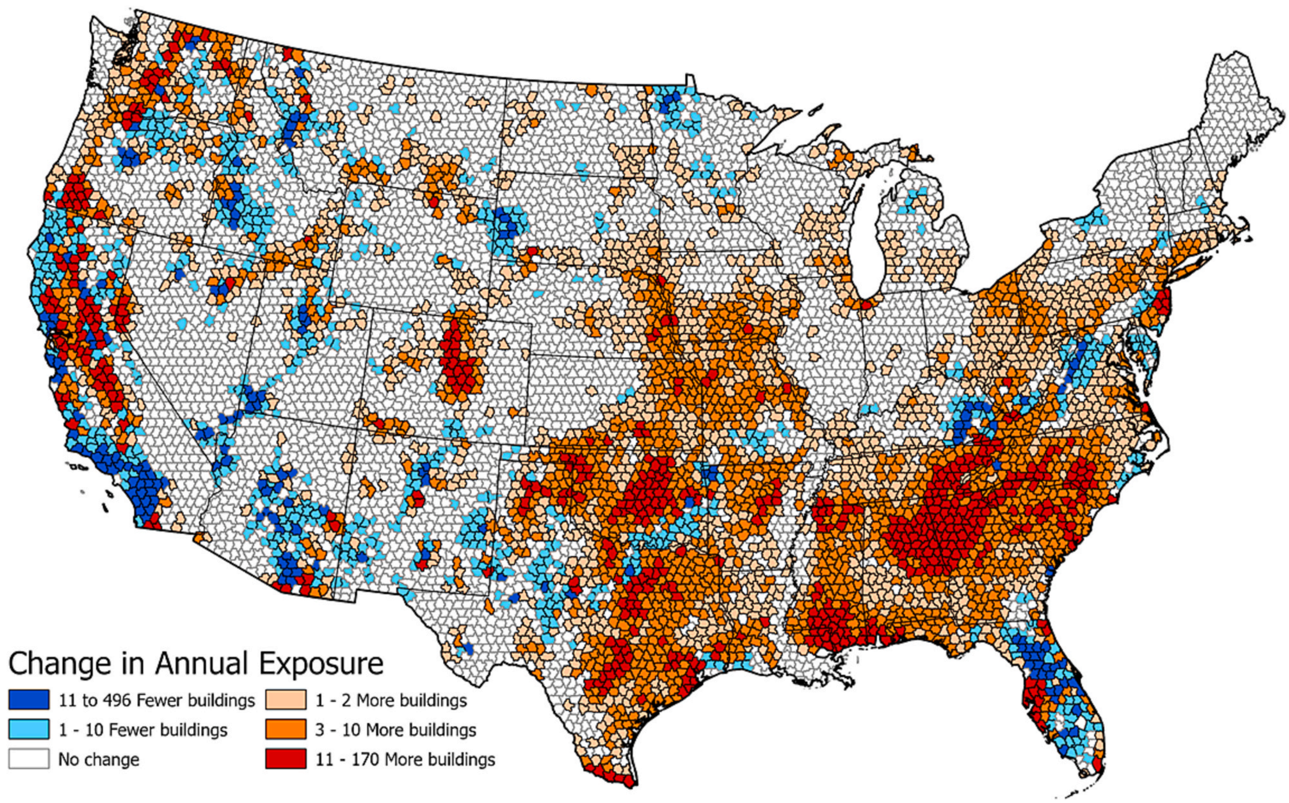

Fig. 5. Spatial patterns of the change in simulated annual building exposure at the fireshed scale (Evers et al. 2021) from the FSim-2020 to the FSim-2023 datasets (Short et al. 2020; Dillon et al. 2023, respectively). See Fig. 1 for data vintages and Table 1 for data sources. Red areas show where simulated annual exposure increased in the FSim-2023 data.

overestimated observed exposure in both the Western US and Eastern US despite many updates to the simulation data and parameters, while annual area burned showed little overestimation. The overestimation was reduced in half (200% to 100%) from the FSim-2020 for the Western US and almost doubled for the Eastern US (493% to 790%). It is interesting to note that the magnitude of the average annual overestimation of building exposure in the Western US for the FSim-2023 simulations (11,676 buildings per year) is less than the 2025 Palisades and Eaton fire that damaged and exposed around ca. 30,000 buildings in 2025, and thus one contemporary extreme event far exceeds the overestimation of exposed buildings in a given year. The overestimation in the simulated exposure exists despite the fact that structure-to-structure combustion in high building density areas generally considered non-burnable are responsible for substantial losses (Mockrin et al., 2023), and are not modeled in FSim.

One plausible explanation is that the FSim suppression model was calibrated based on fire weather (Finney et al., 2025; but see Young et al., 2022), and thus does not account for more effective suppression in developed areas (Baylis and Boomhower, 2023; Gude et al., 2013). Another potential explanation is that the nearest-neighbor resampling of 30-m LANDFIRE fuels to 270-m FSim pixels converts small patches of non-burnable areas with buildings to burnable due to sampling error (there are 81 30-m pixels in one 270-m pixel), thus allowing simulated fires to spread and expose buildings that were located in non-burnable fuels. Cursory analyses (Supplementary Material Table S3, S4) showed that the resampling is responsible for an approximate reduction of non-burnable area from 56% of the total area in CONUS at 30-m resolution to 17% at 270-m resolution. Within the SILVIS WUI, re-sampling to 270 m resulted in a net increase of about 11.9 million buildings from non-burnable pixels to burnable pixels (Supplementary Material Table S4), thus increasing the buildings potentially exposed to fire. This bias could be mitigated by repeating the building-perimeter intersection process (see Methods) and excluding buildings that are on non-burnable LANDFIRE 30-m pixels. By contrast, a factor that probably contributed to the reduction in overestimation in the Western US between simulation versions is the change in the post-processing of FSim-2023 data to exclude islands of non-burnable pixels within perimeters (Supplementary Material Fig. S8). Specifically, in the FSim-2020 data, post processing dissolved non-burnable islands into the enclosing perimeter, potentially adding buildings to the sum of exposed buildings for a particular perimeter.

The return level analysis (Fig. 3) showed that area burned was consistently higher in FSim-2023 for all fire return levels and geographies. Carlson et al. (2025) also reported an increase in area burned between versions, specifically in the proportions of burned area falling in the higher burn probability classes in the western US. They also report a substantially lower proportion of burned area in the low burn probability class in FSim-2023 for the western US. However, we also found that the change in simulated building exposure between the two data sets varied by fire return level. For instance, in CONUS and the Western US, low-occurrence (once every 200 yrs), high building exposure years were substantially reduced in the FSim-2023 data, yet higher for frequent occurrence levels (every 10 yrs) in the East. Given that fire event data are skewed by rare, large fire events and contain a relatively large number of years with no building exposure (Preisler et al., 2004; Schoenberg et al., 2003), we specifically examined differences in the "long-tail" of the distribution (i.e., the 20% of years with the highest building exposure values) by analyzing the exceedance probability of large-scale events (Feller, 1968). Return level plots are a step towards enhancing the interpretation of risk assessment maps that show the average across many simulated fire seasons thus masking the interannual variation in fire activity and the influence of extreme event years and extreme events that account for the bulk of the loss (Abatzoglou et al., 2023; Ager et al., 2021a; Hulse et al., 2016).

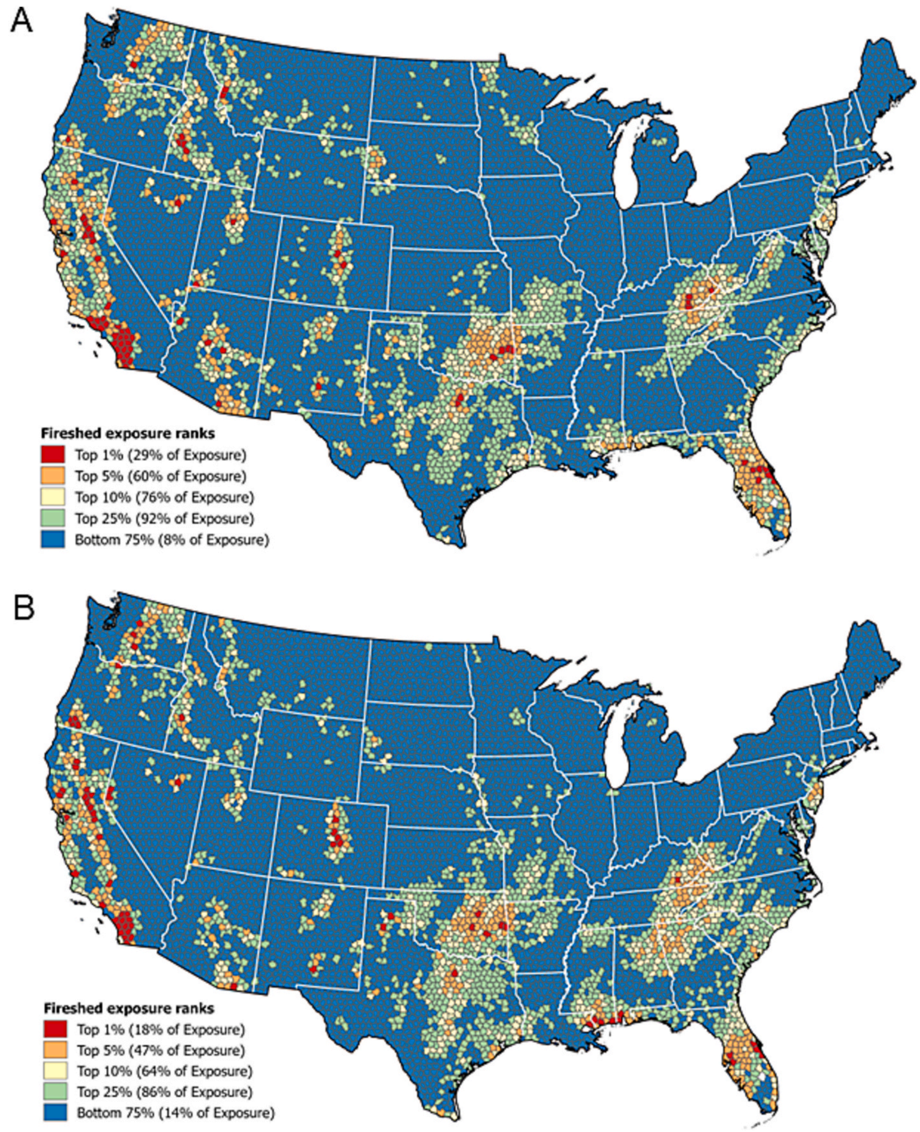

Fig. 6. Fireshed priority ranking based on A) FSim-2020 and B) FSim-2023 annual building exposure summarized at the fireshed scale. Fireshed percentile categories are based on cumulative count (1%, 5%, 10%, 25%, bottom 75%) and were assigned the cumulative simulated building exposure from the firesheds within the respective percentile. For instance, the top ranked 10% of the firesheds in FSim-2020 data accounted for 76% of the total exposure, compared to 64% in the FSim-2023 data.

Table 4
Cumulative building exposure to wildfire (number and percent of total) estimated from the FSim-2020 and FSim-2023 simulations by percent of total area. Firesheds were sorted based on simulated building exposure (highest to lowest) to show potential treatment leverage with increasing treatment area for the two simulations. Data show that, for instance, 5% of the area accounted for 60.4% of the total building exposure in the FSim-2020 simulation versus only 46.7% in the FSim-2023 simulation.

Percent of total area	Cumulative area (million ha)	Cumulative exposure (buildings)			Cumulative exposure (percent of total)		
		FSim-2020	FSim-2023	Diff.	FSim-2020	FSim-2023	Diff.
1	7.7	12,364	9,603	−2,762	28.4	18.2	−10.2
5	38.9	26,298	24,644	−1,653	60.4	46.7	−13.7
10	77.8	33,261	33,869	608	76.4	64.2	−12.2
25	194.7	40,124	45,539	5,415	92.1	86.3	−5.8
100	779.0	43,559	52,751	9,162	100.0	100.0	0.0

In this work we calculated confidence intervals for the return level plots to assess if interannual variation masked the differences between FSim-2020 and FSim-2023 simulations (Fig. 3) and found that a sample of 10,000 fire years resulted in relatively minor confidence intervals owing to the large sample size. In future work, a more meaningful variability assessment from a manager's perspective would be based on a pooled variance calculated from 5-15 years consistent with fuel treatment cycles on federal forests. For instance, return level analyses could be widely applied to understand the effects of fuel management on fire behavior with confidence intervals based on the interannual variation in fire activity during the lifespan (e.g., 5–20 year) of fuel treatments. This approach would provide for testing of statistical significance

Table 5
Regression coefficients for drivers of annual building exposure differences between the FSim-2020 and FSim-2023 wildfire simulations at the fireshed scale across the conterminous US (CONUS), Western and Eastern US.

	CONUS			Western			Eastern		
	Estimate	t-value	*p*	Estimate	t-value	*p*	Estimate	t-value	*p*
Intercept	0.47	11.93	<0.01	0.23	8.06	<0.01	0.58	10.57	<0.01
Base building exposure[a]	−0.68	−49.48	<0.01	−0.38	−27.75	<0.01	−0.97	−44.05	<0.01
Δ ignition frequency	0.31	16.23	<0.01	0.08	2.22	0.03	0.24	10.17	<0.01
Δ burn probability	0.15	12.02	<0.01	0.25	18.99	<0.01	0.07	3.63	<0.01
Δ building counts	0.10	16.34	<0.01	0.09	15.22	<0.01	0.14	8.51	<0.01
Δ grass fuels	0.00	−0.04	0.97	−0.01	−0.57	0.57	−0.01	−0.85	0.40
Δ timber fuels	0.00	−0.4	0.69	−0.01	−1.2	0.23	−0.01	−0.70	0.48
Δ shrub fuels	−0.01	−0.86	0.39	−0.02	−1.85	0.06	0.00	−0.2	0.84
Δ non-burnable fuels	−0.01	−1.8	0.07	0.00	−0.62	0.54	−0.01	−1.16	0.25
Lamda	0.87	137.76	<0.01	0.68	39.04	0.00	0.87	110.07	<0.01
Log-likelihood	−5503.3			−1477.6			−3621.1		
AIC	11,029			2977			7264		
Residual variance	0.45			0.38			0.47		
Moran-I		−4.52	1.0		−1.46	0.93		−3.79	1.0

[a] Controls for underlying differences in magnitude of building exposure by fireshed.

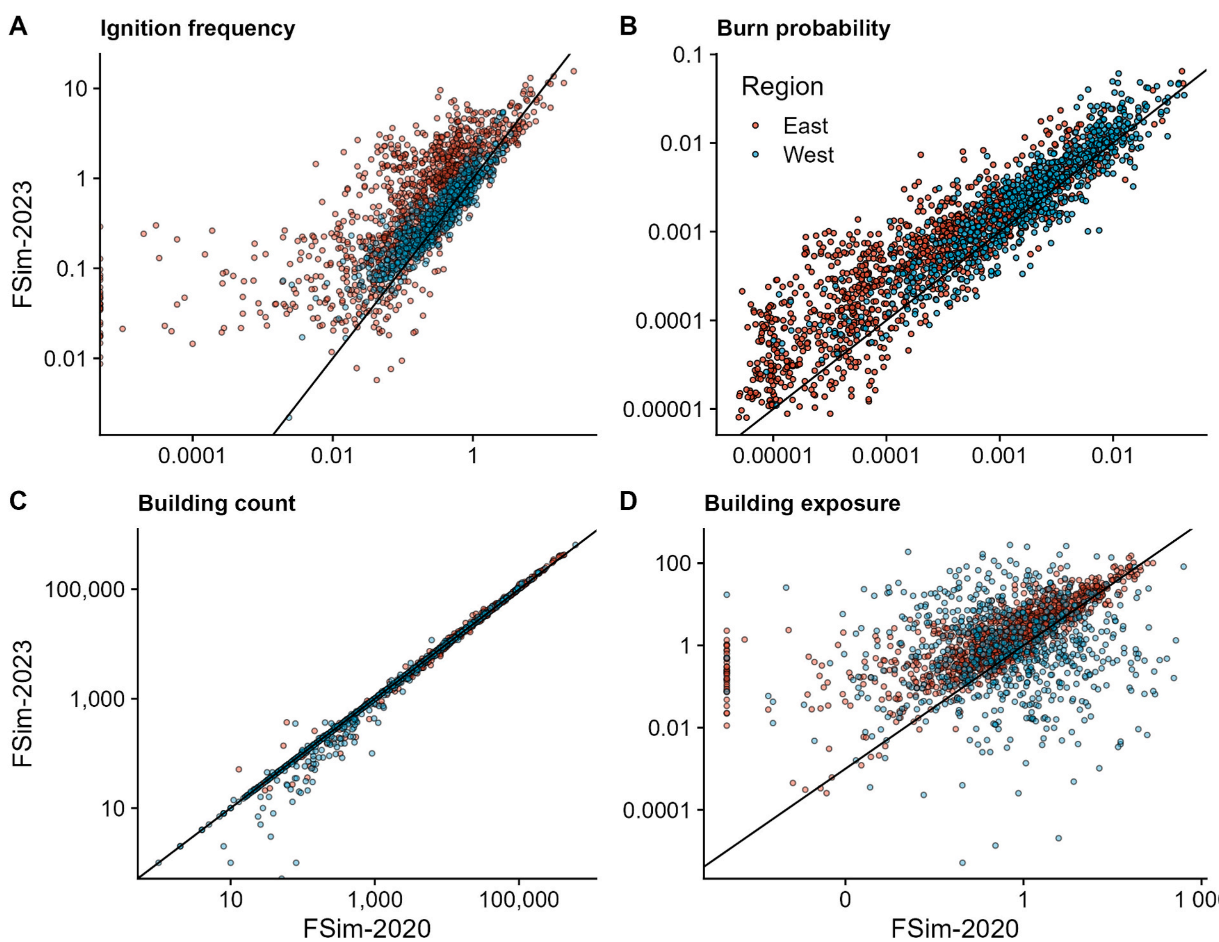

Fig. 7. Comparison of wildfire simulation inputs and outputs at the fireshed scale for the FSim-2020 and FSim-2023 datasets. Scatterplots show average fireshed values for (A) annual burn probability, (B) annual ignition frequency, (C) building count, and (D) annual building exposure for the FSim-2020 and FSim-2023 datasets. Symbols are color coded by Eastern or Western region. Non-burnable areas were excluded from the calculations. All axes are log10 transformed. Observations above the diagonal line represent an increase in values for the FSim-2023 data set and below the line indicate a decrease from FSim-2020.

and how the average change in risk from treatments varied by return levels as demonstrated here for the two different simulation datasets. Despite a large body of literature and review articles with more than a hundred publications dealing with uncertainty and risk in forest planning (Tato et al., 2013; Yousefpour et al., 2012), quantifying the specific effects of interannual variability on short-term risk estimates has received little attention. Prior discussions of wildfire uncertainty have focused on other aspects including the effects of imperfect knowledge about input data and model parameters on fire spread simulations (Benali et al., 2016; Chuvieco et al., 2023).

Our assessment of the factors associated with this change suggest that some of the updates to the input data, including fuels, weather, and ignition frequency, contributed to the changes in simulated building exposure, but not consistently among sub-CONUS geographies, especially firesheds. The substantial increase in exposure in many firesheds was most closely related to increases in ignition frequency driven mostly by patterns in the East, whereas burn probability was most associated with increases in the West. The regional contrast is consistent with broad differences in fire regimes and human development patterns and suggests spread-related controls (and hence fire size) are more important to exposure in the West whereas building exposure in the East is more strongly tied to ignition pressures, human-caused ignitions, and more expansive WUI. Changes in mapped fuels were complex and not consistently related to increases or decreases in building exposure among firesheds. Thus, we conclude that the interactive effects of the updates to the many input data including fire weather (fuel moisture, wind speed, energy release component), and the process of re-calibration of area burned to a more recent period of observed area burned all contributed to the increase in building exposure estimates with the impact of fuels particularly complex (see Supplementary Material for detailed maps for example firesheds). Disentangling the drivers of the change in building exposure was not the primary objective of the study, and would require rerunning FSim for a large number of orthogonal contrasts where inputs are constant except the one variable of interest (fuels, weather, ignitions) as done in Parisien et al. (2010). Even with perfect orthogonal contrasts among the input variables, Parisien et al. (2010) concluded that "in light of natural complexity, it would be extremely difficult to successfully partition the relative contribution of environmental factors in real landscapes." However, the newer simulation outputs do reflect recognized changes to fire regimes in the US under increasingly warmer climate and droughts (Richardson et al., 2022; Westerling et al., 2006), particularly in the Western US.

In conclusion, large-fire simulations remain essential tools for assessing the wildfire risk landscape and will continue to underpin management, mitigation, insurance, and prioritization decisions. Overall, the results here support continued use for broad scale prioritization (e.g., ranking firesheds) by the USFS, but not for assessing absolute building exposure at local community scales with fire perimeters and burn probability in the WUI. The consistent overestimation of building exposure highlights a key limitation in the current FSim simulation outputs for estimating risk in the built environment and reflects the complexity of modeling fire spread, behavior and suppression effectiveness with a large fire simulation model at a relatively coarse resolution relative to building footprints. One could argue that FSim perimeters were never intended to support parcel-level exposure or loss analysis, although the simulation outputs are widely used by federal, state, and local agencies, utilities, and insurance providers to assess community vulnerability and guide mitigation funding. This creates a growing disconnect between the intended scale of the simulations and the scale at which they are being operationalized. The use of existing FSim outputs by federal, state, and local agencies, utilities, and insurance providers (BLM, 2024; Bunzel et al., 2023; Dillon, 2023; Oregon Department of Forestry, 2006; USDA Forest Service, 2024; USGS, 2024; Zuzak et al., 2023) should be aware of the limitations reported in this study to assess community vulnerability particularly in relation to WUI archetypes (see Evers et al. 2019) that differ in structure density, access, and fuel configuration. It is important to note that the limitations we discuss pertain to assessing risk and exposure to features at the scale of building footprints that occur in mosaics of burnable/nonburnable LANDFIRE 30-m pixels. Assessing the risk and the effects of fuel management for coarser grain features (e.g., old growth dependent species, municipal watersheds, carbon) on landscapes dominated by burnable fuels would not be affected by the re-classification bias discussed here.

In the future, rapid changes in risk driven by nonstationary fire regimes and extreme events highlight the need for continued improvement in risk models and supporting data. Recent history has shown that even the most current assessments are predicting yesterday's risk, and decisions based on them carry substantial risk themselves. The co-development of adaptive policy and prioritization frameworks and wider use of scenario analyses that focus on future fire regimes and extreme rare wildfire events can help close the gap between risk assessment products and current trends in wildfire disasters.

CRediT authorship contribution statement

Alan A. Ager: Writing – review & editing, Writing – original draft, Validation, Methodology, Investigation, Funding acquisition, Formal analysis, Conceptualization. **Michelle A. Day:** Writing – review & editing, Writing – original draft, Visualization, Validation, Software, Project administration, Methodology, Investigation, Funding acquisition, Formal analysis, Data curation, Conceptualization. **Cody R. Evers:** Writing – review & editing, Writing – original draft, Visualization, Validation, Methodology, Investigation, Formal analysis, Data curation, Conceptualization. **John B. Kim:** Writing – review & editing, Writing – original draft, Funding acquisition. **Becky K. Kerns:** Writing – review & editing, Writing – original draft, Funding acquisition. **Chris D. Ringo:** Writing – review & editing, Visualization, Data curation.

Declaration of competing interest

The authors declare that they have no known competing financial interests or personal relationships that could have appeared to influence the work reported in this paper.

Acknowledgements

We thank Ken Bunzel for help with geoprocessing to calculate building exposure. We thank Chris Carlson, Greg Dillon, Mark Finney, and anonymous reviewers for valuable feedback on a prior version of the manuscript. This research was supported by the US Department of Agriculture Forest Service, Pacific Northwest Research Station and Rocky Mountain Research Station. The findings and conclusions in this publication are those of the authors and should not be construed to represent any official USDA or U.S. Government determination or policy.

Appendix A. Supplementary data

Supplementary data to this article can be found online at https://doi.org/10.1016/j.landurbplan.2026.105695.

Data availability

Data will be made available on request.

References

Abatzoglou, J., Kolden, C., Williams, A., Sadegh, M., Balch, J., & Hall, A. (2023). Downslope wind-driven fires in the Western United States. *Earth's Future, 11*(5), Article e2022EF003471.

Abatzoglou, J. T., Battisti, D. S., Williams, A. P., Hansen, W. D., Harvey, B. J., & Kolden, C. A. (2021). Projected increases in western US forest fire despite growing fuel constraints. *Communications Earth & Environment, 2*(1), 227.

Adams, M. A., & Neumann, M. (2024). Perspective: Flawed assumptions behind analysis of litter decomposition, steady state and fire risks in Australia. *Forest Ecology and Management, 556*, Article 121741.

Ager, A. A., Day, M. A., Alcasena, F. J., Evers, C. R., Short, K. C., & Grenfell, I. (2021). Predicting Paradise: Modeling future wildfire disasters in the western US. *Science of the Total Environment, 784*, Article 147057. https://doi.org/10.1016/j.scitotenv.2021.147057

Ager, A. A., Day, M. A., Ringo, C., Evers, C. R., Alcasena, F. J., Houtman, R., Scanlon, M., and Ellersick, T. (2021b). *Development and application of the Fireshed Registry*. (Gen. Tech. Rep. RMRS-GTR-425). Fort Collins, CO - USDA Forest Service, Rocky Mountain Research Station. https://www.fs.usda.gov/treesearch/pubs/62641.

Ager, A. A., Evers, C. R., Day, M. A., Alcasena, F. J., & Houtman, R. (2021). Planning for future fire: Scenario analysis of an accelerated fuel reduction plan for the western

United States. *Landscape and Urban Planning, 215*, Article 104212. https://doi.org/10.1016/j.landurbplan.2021.104212

Ager, A. A., Finney, M. A., Kerns, B. K., & Maffei, H. (2007). Modeling wildfire risk to northern spotted owl (*Strix occidentalis* caurina) habitat in Central Oregon, USA. *Forest Ecology and Management, 246*, 45–56.

Ager, A. A., Palaiologou, P., Evers, C., Day, M. A., Ringo, C., & Short, K. C. (2019). Wildfire exposure to the wildland urban interface in the western US. *Applied Geography, 111*, Article 102059. https://doi.org/10.1016/j.apgeog.2019.102059

Ager, A. A., Vaillant, N. M., & Finney, M. A. (2011). Integrating fire behavior models and geospatial analysis for wildland fire risk assessment and fuel management planning. *Journal of Combustion, 572452*, 19. https://doi.org/10.1155/2011/572452

Alcasena, F., Ager, A., Le Page, Y., Bessa, P., Loureiro, C., & Oliveira, T. (2021). Assessing wildfire exposure to communities and protected areas in Portugal. *Fire, 4*(4), 82. https://doi.org/10.3390/fire4040082

Alcasena, F. J., Ager, A. A., Bailey, J. D., Pineda, N., & Vega-Garcia, C. (2019). Towards a comprehensive wildfire management strategy for Mediterranean areas: Framework development and implementation in Catalonia, Spain. *Journal of Environmental Management, 231*, 303–320. https://doi.org/10.1016/j.jenvman.2018.10.027

Alcasena, F. J., Ager, A. A., Salis, M., Day, M. A., & Vega-Garcia, C. (2018). Wildfire spread, hazard and exposure metric raster grids for central Catalonia. *Data in Brief, 17*, 1–5. https://doi.org/10.1016/j.dib.2017.12.069i

Auer, M. R. (2024). Wildfire risk and insurance: Research directions for policy scientists. *Policy Sciences*, 1–26.

Baylis, P., & Boomhower, J. (2023). The economic incidence of wildfire suppression in the United States. *American Economic Journal: Applied Economics, 15*(1), 442–473.

Benali, A., Ervilha, A. R., Sá, A. C., Fernandes, P. M., Pinto, R. M., Trigo, R. M., & Pereira, J. M. (2016). Deciphering the impact of uncertainty on the accuracy of large wildfire spread simulations. *Science of the Total Environment, 569*, 73–85.

Berchtold, C., Plana, E., Saura, J. C., Kalapodis, N., Sakkas, G., Handmer, J., Linnerooth-Bayer, J., Scolobig, A., Tsaloukidis, J., & Ballereau, D. (2025). Disaster risk management tipping points: Impacts of extreme wildfire events and the resulting need for layered disaster risk management solutions. *International Journal of Disaster Risk Reduction, 105894*. https://doi.org/10.1016/j.ijdrr.2025.105894

Bivand, R., & Piras, G. (2015). Comparing implementations of estimation methods for spatial econometrics. *Journal of statistical software, 63*, 1–36.

BLM. (2024). *BLM Fire Risk Assessment*, Retrieved from - https://blm-egis.maps.arcgis.com/apps/MapSeries/index.html?appid=b1fdb5d7d9a34c29a4b1f4850a05c0fc.

Bradshaw, L. S., Deeming, J. E., Burgan, R. E., and Cohen, J. D. (1983). The 1978 National Fire-Danger Rating System: Technical documentation (pp. 44). Ogden, UT - USDA Forest Service, Intermountain Forest and Range Experiment Station.

Braziunas, K. H., Seidl, R., Rammer, W., & Turner, M. G. (2020). Can we manage a future with more fire? Effectiveness of defensible space treatment depends on housing amount and configuration. *Landscape Ecology, 1–22*. https://doi.org/10.1007/s10980-020-01162-x

Bunzel, K., Ager, A. A., Day, M. A., Ringo, C., and Evers, C. (2023). *Smoothed raster of wildfire transmission to buildings in the continental United States and Alaska (3rd Edition)*, Retrieved from - https://doi.org/10.2737/RDS-2022-0015-3.

Bunzel, K., Ager, A. A., Day, M. A., Ringo, C., and Evers, C. (2026). *Smoothed rasters of wildfire transmission to buildings in the continental United States and Hawaii. 4rd Edition.*, Retrieved from - https://doi.org/10.2737/RDS-2022-0015-4.

Carlson, A. R., Hawbaker, T. J., Bair, L. S., Hoffman, C. M., Meldrum, J. R., Baggett, L. S., & Steblein, P. F. (2025). Evaluating a simulation-based wildfire burn probability map for the conterminous US. *International Journal of Wildland Fire, 34*(1).

Chen, B., Wu, S., Jin, Y., Song, Y., Wu, C., Venevsky, S., Xu, B., Webster, C., & Gong, P. (2024). Wildfire risk for global wildland–urban interface areas. *Nature Sustainability, 7*(4), 474–484.

Chuvieco, E., Yebra, M., Martino, S., Thonicke, K., Gómez-Giménez, M., San-Miguel, J., Oom, D., Velea, R., Mouillot, F., & Molina, J. R. (2023). Towards an integrated approach to wildfire risk assessment: When, where, what and how may the landscapes burn. *Fire, 6*(5), 215. https://doi.org/10.3390/fire6050215

Coles, S., Bawa, J., Trenner, L., & Dorazio, P. (2001). *An introduction to statistical modeling of extreme values*. Springer.

Cruz, M. G., & Alexander, M. E. (2013). Uncertainty associated with model predictions of surface and crown fire rates of spread. *Environmental Modelling & Software, 47*, 16–28. https://doi.org/10.1016/j.envsoft.2013.04.004

Dillon, G. K. (2023). *Wildfire Hazard Potential (WHP) for the conterminous United States (270-m), version 2023*, Retrieved from – doi: 10.2737/RDS-2015-0047-4.

Dillon, G. K. (2024). *Wildfire Hazard Potential for the United States (270-m), version 2023 (4th Edition)*, Retrieved from - https://doi.org/10.2737/RDS-2015-0047-4.

Dillon, G. K., Scott, J. H., Jaffe, M. R., Olszewski, J. H., Vogler, K. C., Finney, M. A., Short, K. C., Riley, K. L., Grenfell, I. C., Jolly, W. M., and Brittain, S. (2023). *Spatial datasets of probabilistic wildfire risk components for the United States (270m)*, Retrieved from – doi: 10.2737/RDS-2016-0034-3.

Dye, A. W., Gao, P., Kim, J. B., Lei, T., Riley, K. L., & Yocom, L. (2023). High-resolution wildfire simulations reveal complexity of climate change impacts on projected burn probability for Southern California. *Fire Ecology, 19*(1), 1–19.

Dye, A. W., Houtman, R. M., Gao, P., Anderegg, W. R., Fettig, C. J., Hicke, J. A., Kim, J. B., Still, C. J., Young, K., & Riley, K. L. (2024). Carbon, climate, and natural disturbance: A review of mechanisms, challenges, and tools for understanding forest carbon stability in an uncertain future. *Carbon Balance and Management, 19*(1), 35. https://doi.org/10.1186/s13021-024-00282-0

Dye, A. W., Kim, J. B., McEvoy, A., Fang, F., & Riley, K. L. (2021). Evaluating rural Pacific Northwest towns for wildfire evacuation vulnerability. *Natural Hazards*. https://doi.org/10.1007/s11069-021-04615-x

Essen, M., McCaffrey, S., Abrams, J., & Paveglio, T. (2023). Improving wildfire management outcomes: Shifting the paradigm of wildfire from simple to complex risk. *Journal of Environmental Planning and Management, 66*(5), 909–927.

Evers, C., Ager, A. A., Nielsen-Pincus, M., Palaiologou, P., & Bunzel, K. (2019). Archetypes of community wildfire exposure from national forests in the western US. *Landscape and Urban Planning, 182*, 55–66. https://doi.org/10.1016/j.landurbplan.2018.10.004

Evers, C., Ringo, C., Ager, A. A., Day, M. A., Alcasena, F. J., and Bunzel, K. (2024). *The Fireshed Registry: Fireshed and subfireshed boundaries for the continental United States and Alaska (3rd Edtion)*, Retrieved from - https://doi.org/10.2737/RDS-2020-0054-3.

Feller, W. (1968). *An introduction to probability theory and its applications*. New York - John Wiley and Sons.

Finney, M. A. (2002). Fire growth using minimum travel time methods. *Canadian Journal of Forest Research, 32*(8), 1420–1424. https://doi.org/10.1139/x02-068

Finney, M. A. (2005). The challenge of quantitative risk analysis for wildland fire. *Forest Ecology and Management, 211*(1–2), 97–108. https://doi.org/10.1016/j.foreco.2005.02.010

Finney, M. A., Grenfell, I. C., & McHugh, C. W. (2009). Modeling containment of large wildfires using generalized linear mixed model analysis. *Forest Science, 55*(3), 249–255.

Finney, M. A., McHugh, C. W., Grenfell, I. C., Riley, K. L., & Short, K. C. (2011). A simulation of probabilistic wildfire risk components for the continental United States. *Stochastic Environmental Research and Risk Assessment, 25*, 973–1000. https://doi.org/10.1007/s00477-011-0462-z

Finney, M. A., Zimmer, S. N., Riley, K. L., & Grenfell, I. C. (2025). A generalized wildfire containment algorithm. *Ecological Modelling, 505*, Article 111134. https://doi.org/10.1016/j.ecolmodel.2025.111134

First Street Technology. (2024). *Fire Factor wildfire risk model methodology*, Retrieved from - https://firststreet.org/methodology/fire.

Gilleland, E., & Katz, R. W. (2016). extRemes 2.0: An extreme value analysis package in R. *Journal of Statistical Software, 72*, 1–39.

Gude, P. H., Jones, K., Rasker, R., & Greenwood, M. C. (2013). Evidence for the effect of homes on wildfire suppression costs. *International Journal of Wildland Fire, 22*(4), 537–548.

Hamilton, M., Evers, C., Nielsen-Pincus, M., & Ager, A. (2024). Matching the scales of planning and environmental risk: An evaluation of Community Wildfire Protection Plans in the western US. *Regional Environmental Change, 24*(2), 93.

Hazra, D., & Gallagher, P. (2022). Role of insurance in wildfire risk mitigation. *Economic Modelling, 108*, Article 105768.

Hulse, D., Branscomb, A., Enright, C., Johnson, B., Evers, C., Bolte, J., & Ager, A. (2016). Anticipating surprise: Using agent-based alternative futures simulation modeling to identify and map surprising fires in the Willamette Valley, Oregon USA. *Landscape and Urban Planning, 156*, 26–43.

Jones, M. W., Abatzoglou, J. T., Veraverbeke, S., Andela, N., Lasslop, G., Forkel, M., Smith, A. J., Burton, C., Betts, R. A., and van der Werf, G. R. (2022). Global and regional trends and drivers of fire under climate change. *Reviews of Geophysics*, *60* (3), e2020RG000726. doi - 10.1029/2020RG000726.

Lambert, J. H., Matalas, N. C., Ling, C. W., Haimes, Y. Y., & Li, D. (1994). Selection of probability distributions in characterizing risk of extreme events. *Risk Analysis, 14* (5), 731–742.

LANDFIRE. (2017). *40 Scott and Burgan Fire Behavior Fuel Models. LF 1.4.0. Refresh.*, Retrieved from - https://www.landfire.gov/fbfm40.php.

LANDFIRE. (2020). *40 Scott and Burgan Fire Behavior Fuel Models. LF 2020 [LF 2.2.0]*, Retrieved from - https://www.landfire.gov/fbfm40.php.

McEvoy, A., Dunn, C., and Rickert, I. (2023). *PNW Quantitative Wildfire Risk Assessment methods*. (Unpublished manuscript USDA Forest Service, Oregon State University. https://oe.oregonexplorer.info/externalcontent/wildfire/PNW_QWRA_2023Methods.pdf.

McEvoy, A., Kerns, B. K., & Kim, J. B. (2021). Hazards of risk: Identifying plausible community wildfire disasters in low-frequency fire regimes. *Forests, 12*(7). https://doi.org/10.3390/f12070934

Microsoft. (2018). *Computer generated building footprints for the United States GitHub repository*, Retrieved 21 February 2022 from - https://github.com/Microsoft/USBuildingFootprints.

Microsoft. (2020). *Computer generated building footprints for the United States GitHub repository*, Retrieved 21 February 2022 from - https://github.com/Microsoft/USBuildingFootprints.

Mills, D., Jones, R., Wobus, C., Ekstrom, J., Jantarasami, L., St Juliana, A., & Crimmins, A. (2018). Projecting age-stratified risk of exposure to inland flooding and wildfire smoke in the United States under two climate scenarios. *Environmental Health Perspectives, 126*(4), Article 047007. https://doi.org/10.1289/EHP2594

Mockrin, M. H., Locke, D. H., Syphard, A. D., & O'Neil-Dunne, J. (2023). Using high-resolution land cover data to assess structure loss in the 2018 Woolsey Fire in Southern California. *Journal of Environmental Management, 347*, Article 118960. https://doi.org/10.1016/j.jenvman.2023.118960

MTBS. (2020). *MTBS Data Access: Burned areas boundaries, 1984-2018*, Retrieved 6 November 2020 from - https://www.mtbs.gov/index.php/direct-download.

MTBS. (2024). *MTBS Data Access: Burned areas boundaries, 1984-2020*, Retrieved from - https://www.mtbs.gov/index.php/direct-download.

Naser, M., & Kodur, V. (2025). Vulnerability of structures and infrastructure to wildfires: A perspective into assessment and mitigation strategies. *Natural Hazards, 121*(8), 9995–10015.

NOAA. (2023). *Monthly wildfires report for Annual 2022*. National Centers for Environmental Information. https://www.ncei.noaa.gov/access/monitoring/monthly-report/fire/202213.

Oliveira, S., Rocha, J., & Sá, A. (2021). Wildfire risk modeling. *Current Opinion in Environmental Science & Health, 23*, Article 100274. https://doi.org/10.1016/j.coesh.2021.100274

Oregon Department of Forestry. (2006). *Oregon Explorer Wildfire Risk*, Retrieved January 29 2025 from - https://hub.oregonexplorer.info/pages/wildfire.

Palaiologou, P., Kalabokidis, K., Day, M. A., Ager, A. A., Galatsidas, S., & Papalampros, L. (2022). Modelling fire behavior to assess community exposure in Europe: Combining open data and geospatial analysis. *International Journal of Geo-Information, 11*(3), 198. https://doi.org/10.3390/ijgi11030198

Parisien, M.-A., Ager, A. A., Barros, A. M., Dawe, D., Erni, S., Finney, M. A., McHugh, C. W., Miller, C., Parks, S. A., Riley, K. L., Short, K. C., Stockdale, C. A., Wang, X., and Whitman, E. (2020a). Commentary on the article "Burn probability simulation and subsequent wildland fire activity in Alberta, Canada – Implications for risk assessment and strategic planning" by J.L. Beverly and N. McLoughlin. *Forest Ecology and Management*, *460*, doi - 10.1016/j.foreco.2019.117698.

Parisien, M. A., Barber, Q. E., Hirsch, K. G., Stockdale, C. A., Erni, S., Wang, X., Arseneault, D., & Parks, S. A. (2020). Fire deficit increases wildfire risk for many communities in the Canadian boreal forest. *Nature Communications, 11*(1), 2121. https://doi.org/10.1038/s41467-020-15961-y

Parisien, M. A., Miller, C., Ager, A. A., & Finney, M. A. (2010). Use of artificial landscapes to isolate controls on burn probability. *Landscape Ecology, 25*, 79–93.

Preisler, H. K., Brillinger, D. R., Burgan, R. E., & Benoit, J. W. (2004). Probability based models for estimation of wildfire risk. *International Journal of Wildland Fire, 13*(2), 133–142. https://doi.org/10.1071/Wf02061

Price, O., Borah, R., Bradstock, R., & Penman, T. (2015). An empirical wildfire risk analysis: The probability of a fire spreading to the urban interface in Sydney, Australia. *International Journal of Wildland Fire, 24*(5), 597–606. https://doi.org/10.1071/WF14160

Richardson, D., Black, A. S., Irving, D., Matear, R. J., Monselesan, D. P., Risbey, J. S., Squire, D. T., and Tozer, C. R. (2022). Global increase in wildfire potential from compound fire weather and drought. *npj Climate and Atmospheric Science*, *5*(1), 23. doi - 10.1038/s41612-022-00248-4.

Riley, K. L., Zimmer, S. N., Kodra, E., Grenfell, I. C., Dillon, G. K., Scott, J. H., Jaffe, M. R., Olszewski, J. H., Vogler, K. C., Finney, M. A., Short, K. C., Jolly, W. M., Brittain, S., and Callahan, M. N. (2025). *Spatial datasets of probabilistic wildfire risk components for the conterminous United States (270m) for circa 2011 climate and project future climate circa 2047*, Retrieved from - https://doi.org/10.2737/RDS-2025-0006.

Sajjad, M., Lin, N., and Chan, J. C. L. (2020). Spatial heterogeneities of current and future hurricane flood risk along the U.S. Atlantic and Gulf coasts. *Science of the Total Environment*, *713*, 136704. doi - 10.1016/j.scitotenv.2020.136704.

Salis, M., Arca, B., Del Giudice, L., Palaiologou, P., Alcasena-Urdiroz, F., Ager, A., Fiori, M., Pellizzaro, G., Scarpa, C., Schirru, M., Ventura, A., Casula, M., & Duce, P. (2021). Application of simulation modeling for wildfire exposure and transmission assessment in Sardinia, Italy. *International Journal of Disaster Risk Reduction, 58*, Article 102189. https://doi.org/10.1016/j.ijdrr.2021.102189

Santo, A. R., Huber-Stearns, H., & Smith, H. (2022). Communicating with the public about wildland fire preparation, response, and recovery: A review of recent literature. *Applied Environmental Education & Communication, 21*(4), 383–405.

Schoenberg, F. P., Peng, R., & Woods, J. (2003). On the distribution of wildfire sizes. *Environmetrics, 14*(6), 583–592.

Scott, J. H., Dillon, G. K., Jaffe, M. R., Vogler, K. C., Olszewski, J. H., Callahan, M. N., Karau, E. C., Lazarz, M. T., Short, K. C., Riley, K. L., Finney, M. A., and Grenfell, I. C. (2024). *Wildfire Risk to Communities: Spatial datasets of landscape-wide wildfire risk components for the United States (2nd Edition)*, Retrieved from - https://doi.org/10.2737/RDS-2020-0016-2.

Scott, J. H., Gilbertson-Day, J. W., Moran, C., Dillon, G. K., Short, K. C., and Vogler, K. C. (2020). *Wildfire Risk to Communities: Spatial datasets of landscape-wide wildfire risk components for the United States*, Retrieved from - https://doi.org/10.2737/RDS-2020-0016.

Short, K. C. (2017). *Spatial wildfire occurrence data for the United States, 1992-2015 [FPA_FOD_20170508]. (4th Edition)*, Retrieved 30 July 2018 from - https://doi.org/10.2737/RDS-2013-0009.4.

Short, K. C. (2022). *Spatial wildfire occurrence data for the United States, 1992-2020 [FPA_FOD_20221014] (6th Edition)*, Retrieved 38 March 2022 from - https://doi.org/10.2737/RDS-2013-0009.6.

Short, K. C., Finney, M. A., Vogler, K., Scott, J. H., Gilbertson-Day, J. W., Julie, W., and Grenfell, I. C. (2020a). *Spatial datasets of probabilistic wildfire risk components for the United States (270m)*, Retrieved 14 March 2016 from - https://doi.org/10.2737/RDS-2016-0034-2.

Short, K. C., Grenfell, I. C., Riley, K. L., and Vogler, K. (2020b). *Pyromes of the conterminous United States*, Retrieved from - https://doi.org/10.2737/RDS-2020-0020.

St Denis, L. A., Mietkiewicz, N. P., Short, K. C., Buckland, M., & Balch, J. K. (2020). All-hazards dataset mined from the US National Incident Management System 1999-2014. *Scientific Data, 7*(1), 64. https://doi.org/10.1038/s41597-020-0403-0

Tato, M. P., Mäkinen, A., Gonzalo, J. G., Borges, J. G., Lämas, T., & Eriksson, L.-O. (2013). Assessing uncertainly and risk in forest planning and decision support systems: Review of classical methods and introduction of innovative approaches. *Forest Systems, 22*(2), 282–303.

USDA Forest Service. (2022). *Confronting the Wildfire Crisis: A Strategy for Protecting Communities and Improving Resilience in America's Forests*. FS-1187a). Washington D. C. - https://www.fs.usda.gov/sites/default/files/fs_media/fs_document/Confronting-the-Wildfire-Crisis.pdf.

USDA Forest Service. (2024). *Wildfire risk to communities*, Retrieved January 29 2025 from - https://wildfirerisk.org/explore/.

USGS. (2024). *Wildfire hazard and risk assessment clearinghouse*, Retrieved from - https://apps.usgs.gov/wildfire_hazard_and_risk_assessment_clearinghouse/.

Westerling, A. L., Hidalgo, H. G., Cayan, D. R., & Swetnam, T. W. (2006). Warming and earlier spring increase western U.S. forest wildfire activity. *Science, 313*, 940–943. https://doi.org/10.1126/science.1128834

Young, J. D., Ager, A. A., & Thode, A. E. (2022). Using wildfire as a management strategy to restore resiliency to ponderosa pine forests in the southwestern United States. *Ecosphere, 13*, e4040.

Yousefpour, R., Jacobsen, J. B., Thorsen, B. J., Meilby, H., Hanewinkel, M., & Oehler, K. (2012). A review of decision-making approaches to handle uncertainty and risk in adaptive forest management under climate change. *Annals of Forest Science, 69*, 1–15. https://doi.org/10.1007/s13595-011-0153-4

Zuzak, C., Goodenough, E., Stanton, C., Mowrer, M., Sheehan, A., Roberts, B., McGuire, P., and Rozelle, J. (2023). *National Risk Index technical documentation*. Washington, D.C. - Federal Emergency Management Agency. https://hazards.fema.gov/nri/wildfire.